International Journal of GEOMATE, July., 2021, Vol.21, Issue 83, pp.-101-108
ISSN: 2186-2982 (P), 2186-2990 (O), Japan, DOI: https://doi.org/10.21660/2021.83.Gx370
Geotechnique, Construction Materials and Environment

# COMPARISON STUDY ON THE DYNAMIC RESPONSE OF REINFORCED CONCRETE ABUTMENTS

* Desy Setyowulan[1], Toshitaka Yamao[2], Tomohisa Hamamoto[3], Eko Andi Suryo[4], Eva Arifi[5], and Devi Nuralinah[6]

[1,4,5,6]Engineering, Universitas Brawijaya, Indonesia;
[2]Center for Water Cycle, Marine Environment, and Disaster Management, Kumamoto University, Japan
[3]Department of Civil Engineering, Nishinippon Institute of Technology, Fukuoka, Japan

*Corresponding Author, Received: 30 Nov. 2020, Revised: 24 Mar. 2021, Accepted: 04 Apr. 2021

**ABSTRACT:** Abutment performance suggestively impacts the seismic response of bridge constructions. This research investigates the dynamic performance of reinforced concrete abutments in the actual bridge construction with the consequence of the wing wall and movement constraint. The concrete box girder bridge's analytical model was implemented from the actual bridge in Japan, with the numerical model was performed by a 3D finite element model in ABAQUS software. Four distinct abutment modeling approaches were carried out, including abutment without wing wall as Type 1, an ordinary abutment form in Japan as Type 2, abutment with the entire wing wall as Type 3, and the proposed model Type 4. Comparison study will be taken for different positions of input ground acceleration, which were applied horizontally at the bottom of the pier and abutments as Type A, and at the bottom of the pier as Type B. The input seismic motion was Level 2 Type 2 with ground Type I. The results confirmed that the input seismic ground acceleration position resulted in the different response on shear stress and response stress of abutment. The response stress of abutment with 20 cm of the gap is less than 10 cm. Besides, abutment Type 4 has the capability of resisting the flexural load due to strong ground motion.

*Keywords: ABAQUS, Abutment, Seismic Response, Real Bridge Model, Wing Wall*

## 1. INTRODUCTION

The abutment has an important function on the performance of bridge structure because its behavior has been found to significantly impact the response of the whole bridge due to the high intensity of seismic excitation [1]. According to the previous experiences, many abutments collapsed in Japan due to the large stress on the surface of the abutment and pounding between superstructure and substructure.

After the 1995 Hyogo-ken Nanbu Earthquake, the consideration of the 10 cm gap which has been used in the actual bridge in Japan was revised due to numerous damages on bridges suffered by the collision phenomenon. Furthermore, a necessary gap between two adjacent girders or among girder and abutments have to be taken into design of the superstructure for avoiding any damage to the bridge triggered by the collision.

The influence of the pounding effect on the parapet wall of abutment behavior, especially on the deflection, crack and stress-strain result on the parapet wall and steel reinforcement were numerically investigated [2] and experimentally tested [3]. Results show that the crack phenomenon distributes on the bottom of the parapet wall, which propagates along the width of this structure [3]. Also, it was demonstrated that the effect of the wing wall in reducing the displacement of the proposed model was significant in the wing wall part [2].

The substantial effect of parapet-unified wing walls of abutment subjected to horizontal loads through unseating prevention structure of the bridge was studied [4]. According to this analysis, it was found that the bending moment at the base of the parapet was affected by the wing walls. To prove the result of numerical analysis, an experimental model of reinforced concrete parapet wall of abutment without wing wall subjected to incremental horizontal load was inspected previously [3]. From this model, it was found that crack developed on the bottom of the parapet wall and propagate along this wall.

A recent study on cost analysis of the proposed reinforcement method for abutment due to girder's collision was developed, which was modeled by the 3D-Finite Element Method [5]. According to this research, it could be confirmed that the proposed seismic reinforcement method is very effective to be compared with the current method of reinforcement.

Investigation on the seismic response of bridge especially on abutments was analyzed [6]. In that study, the input seismic ground acceleration was applied at the bottom of the pier. Furthermore, this numerical study is developed with seismic ground motion input at the bottom of the pier and abutments

on both sides which correspond to the real situation when an earthquake happened.

## 2. RESEARCH SIGNIFICANCE

Data produced from this study will be used to show the dynamic performance in different RC abutments, with three types of ground motions. This data will be used to determine the type of abutment under the real condition. Also, an appropriate gap can be determined to be used in the real abutment. It is hoped that this research will be the beginning of ongoing research related to the behavior of sub-structure in consequence with liquefaction on the real structure model.

## 3. METHODS

The modeling simulations of reinforced concrete abutments were developed by using three-dimensional solid elements, which were performed with ABAQUS software [7]. The discretization of abutment's geometry, material properties for concrete and steel, applied load, and boundary condition for the structure was addressed.

### 3.1 Finite Element Modeling

The analytical model of the concrete box girder bridge was assumed from the real bridge in Japan, which was conducted previously [6, 2] shown in Fig. 1. The total length of two-span superstructures was 80 m with a pier as its center and abutment in its edges. Earthquake ground motion was applied at the bottom of the pier and abutments on both sides as Type A, as shown in Fig. 1(a). The result will be compared to Type B with input seismic motion at the bottom of the pier, as shown in Fig. 1(b).

Four different abutment modeling approaches shown in Fig. 2 were used as the main parameter of this research. These approaches including Type 1 as abutment without wing wall, Type 2 as an ordinary model in Japan, Type 3 as abutment with full wing wall, and Type 4 as a new type of abutment which is proposed in this research.

The dimensional configurations of the total height, width, and thickness of the wing wall and parapet wall were 8.0 m, 6.0 m, and 0.5 m, respectively, with a length of the wing wall, which was 4.0 m. The gap between superstructures was set to be 10 cm and 20 cm. The bearing supports were assumed as fixed and roller bearings for pier and abutment, respectively. Additionally, the friction coefficient was set to be 0.1.

In this non-linear simulation, the material properties for concrete are shown in Fig. 3(a), with the ultimate strength of 29.4 MPa and 50% of the linear elastic range. The Poisson's ratio and modulus of elasticity were 0.2 and 20.6 GPa, respectively. The compression and tension damaged variables, dc and dt, were defined and plotted in Figs. 3(b) 3(c), respectively. Besides, the reinforcing bars were assumed as steel with Young's modulus, Poisson's ratio, density, and tensile strength of 206 GPa, 0.3, 7850 kg/m3, and 294 MPa.

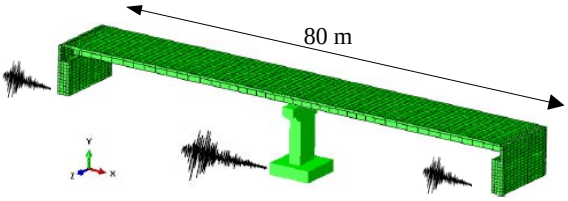


(a) Side view of the bridge as Type A

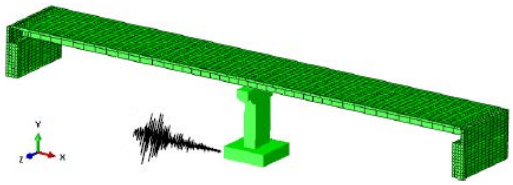

(b) Side view of the bridge as Type B

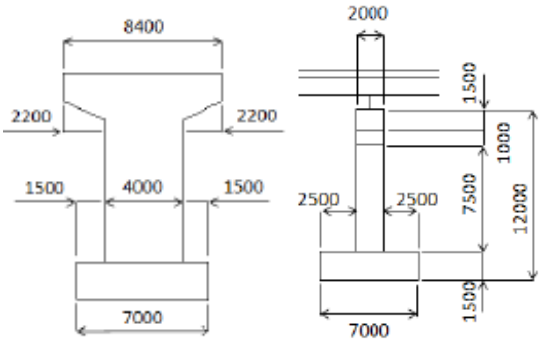


(c) Dimensions of the pier (unit: mm)

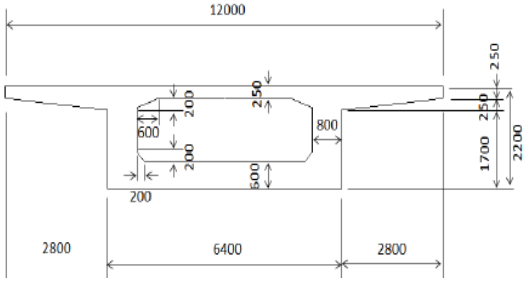


(d) Cross-section of the superstructure (unit: mm)

Fig. 1 Three-dimensional finite element models of concrete girder bridges in ABAQUS with the view of pier and cross-section of superstructure [6, 2]

The method of Concrete Damaged Plasticity was selected due to its superiority in damage simulation. The concrete material of the abutment was formed with the C3D8R element, which is known as eight-node solid (brick) elements. The

concrete materials for column and box girder were idealized by beam element and shell element, respectively. While the reinforcing bar was idealized by 3D truss elements, identified as T3D2. The embedded method was also applied to constraint the two-node truss element (reinforcing bar) into a solid element (concrete) to create a proper bond action [8].

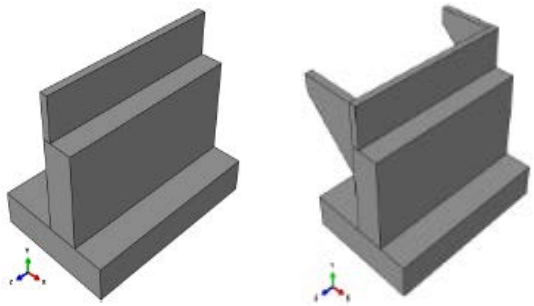

(a) Type 1 (b) Type 2 (standard)

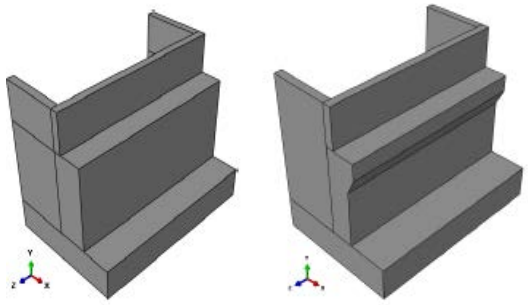

(c) Type 3 (d) Type 4

Fig. 2 Theoretical models of abutments

### 3.2 Input Seismic Wave

Level 2 Type 2 with ground (soil) Type I (L2T2G1) earthquake ground motion with accelerations type were applied horizontally at the lowest part of substructures. It is known as an inland direct strike type earthquake with a low probability of occurrence, which is represented with strong accelerations and shorter duration. Three input seismic waves are shown in Fig. 4. Furthermore, it was assumed that no liquefaction occurred.

### 3.3 Loading

The loading condition for abutment under an earthquake should be designed with the combination of dead loads, earth pressure, and seismic effect [10]. Calculation of the earth's pressure was assumed as a distributed load acting on the backfill of the abutment. The soil properties were determined previously by Yamao et al., 2012. The Monobe-Okabe method was used to calculate an active pressure strength during an earthquake, as determined in Eqs. (1) and (2). PEA and KEA were determined as strength of an active earth pressure ($kN/m^2$) at depth x (m) and coefficient of active earth pressure, respectively.

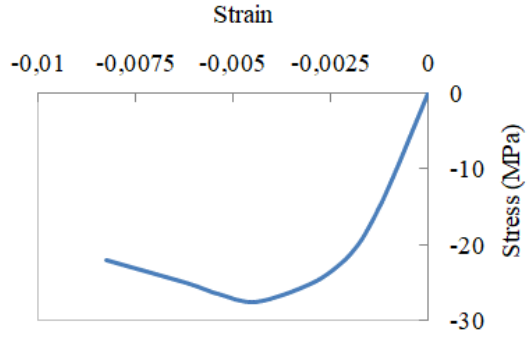


(a) Stress vs strain curve

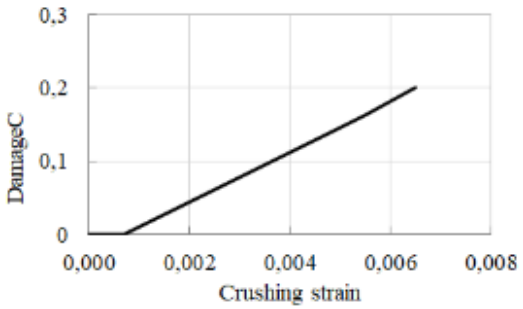


(a) Compression damage

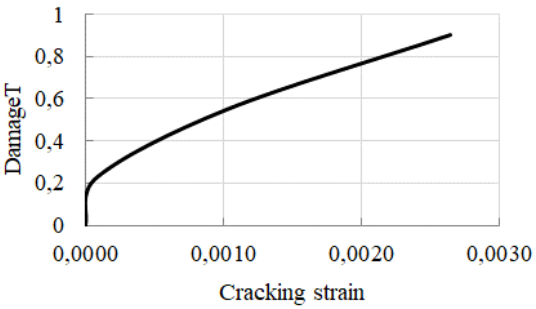


(b) Tension damage

Fig.3 Material properties of the concrete in ABAQUS

$$P_{EA} = r\,K_{EA} + q'K_{EA} \quad (1)$$

$$K_{EA} = \frac{\cos^2(\phi - \theta_o - \theta)}{\cos\theta_o \cos^2\theta \cos(\theta + \theta_o + \delta_E)\left(1 + \sqrt{\frac{\sin(\phi + \delta_E)\sin(\phi - \alpha - \theta_o)}{\cos(\theta + \theta_o + \delta_E)\cos(\theta - \alpha)}}\right)^2} \quad (2)$$

### 3.4 Proposal of the Damage Assessment

The determination of damage in abutment was examined by using allowable stress of concrete [9], as shown in Table 1.

Allowable stress for four different design strengths of concrete is specified. Therefore, allowable shear stresses as the maximum elastic limit and allowable compressive stresses with flexural types were defined as 1.9 MPa and 10.0 MPa. The criteria of damage were divided into minor damage as A level, B, C, and D as extensive damage, which was based on the compressive strength design of the concrete for abutment of 27.5 MPa as shown in Table 2.

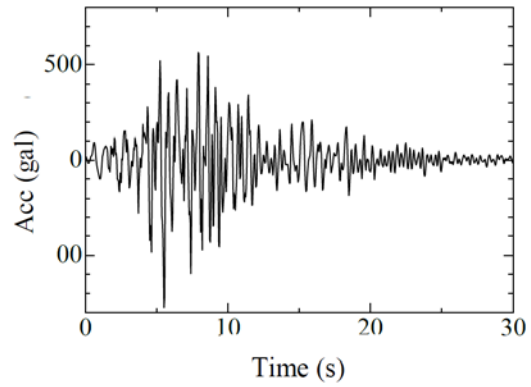


(a) L2T2G1-1

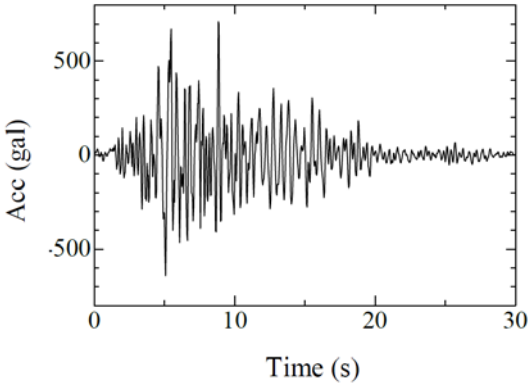


(b) L2T2G1-2

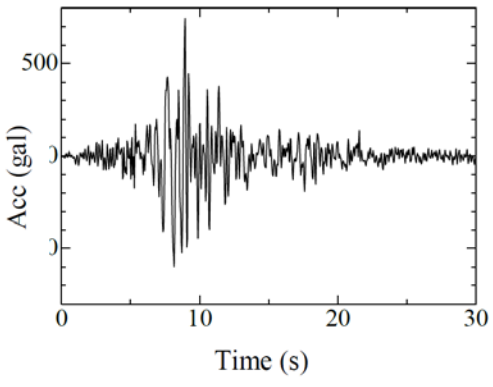


(c) L2T2G1-3

Fig.4 Input seismic wave (L2T2G1) from JSHB seismic waves [9]

Table 1. Allowable stresses of concrete [9]

| Design strengths of concrete (MPa) | | 21 | 24 | 27 | 30 |
|---|---|---|---|---|---|
| Type of stress | | | | | |
| Compres-sive stresses (MPa) | Flexural compressive stresses | 7.0 | 8.0 | 9.0 | 10.0 |
| | Axial compressive stresses | 5.5 | 6.5 | 7.5 | 8.5 |
| | When only concrete carries shear forces $(\tau_{o1})$ | 0.22 | 0.23 | 0.24 | 0.25 |
| Shear stresses (MPa) | When concrete and diagonal tensile reinforcement jointly carry $(\tau_{o2})$ | 1.6 | 1.7 | 1.8 | 1.9 |
| | Punching shear stresses $(\tau_{o3})$ | 0.85 | 0.90 | 0.95 | 1.00 |

Table 2. Level of damage for concrete abutment [6]

| Maximum response stress (MPa) | Level of damage | Description |
|---|---|---|
| $\boldsymbol{0 < \sigma \leq 0,5f'c}$ | A | Minor |
| $\boldsymbol{0,5f'c < \sigma \leq 0,75f'c}$ | B | |
| $\boldsymbol{0,75f'c < \sigma \leq f'c}$ | C | |
| $\boldsymbol{f'c < \sigma}$ | D | Extensive |

## 4. RESULTS AND DISCUSSIONS

Previous studies have reported that the areas subjected to high stress are frequently observed during the investigation of abutment's failure. Furthermore, evaluating the eigenvalue analysis, the shear stress, the response stress, and displacement at abutments are useful to control the damage of abutments.

### 4.1 Eigenvalue Analysis

The dynamic characteristics for box-girder bridge structure in this study were explicitly portrayed through modal analysis procedures by eigenvalue analysis in previous research [6]. From this analysis, it was found the predominant mode was in equal position for the bridge with a different gap of 10 cm and 20 cm. Otherwise; the installation

of four different abutment modeling approaches had a significant effect on its predominant mode, due to the effect of the wing wall. The possibility of a bridge with abutment Type 4 vibrating sympathetically was at the 9th mode in X-direction, 10th mode in Y and Z-direction.

### 4.2 Shear Stresses of Abutments

In this numerical simulation, the maximum shear stress occurred in all abutments with different gap were analyzed. As shown in Fig. 5 for comparison results of Type A and Type B. S1 and S2 denote the position of substructures (abutments) in the left and right side, respectively. According to these figures, it can be seen that abutment Type 2 has the largest value of the shear stress, especially for input seismic motion Type B and 20 cm of the gap.

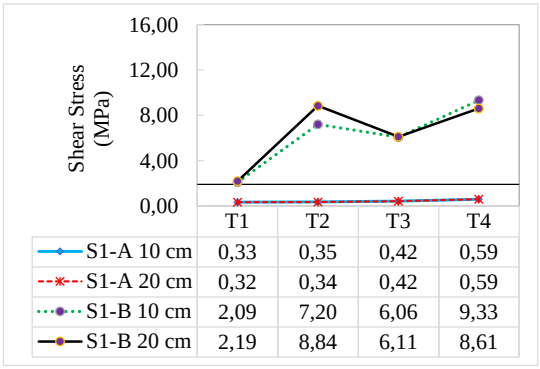


| | T1 | T2 | T3 | T4 |
|---|---|---|---|---|
| S1-A 10 cm | 0,33 | 0,35 | 0,42 | 0,59 |
| S1-A 20 cm | 0,32 | 0,34 | 0,42 | 0,59 |
| S1-B 10 cm | 2,09 | 7,20 | 6,06 | 9,33 |
| S1-B 20 cm | 2,19 | 8,84 | 6,11 | 8,61 |

(a1) S1 (L2T2G1-1)

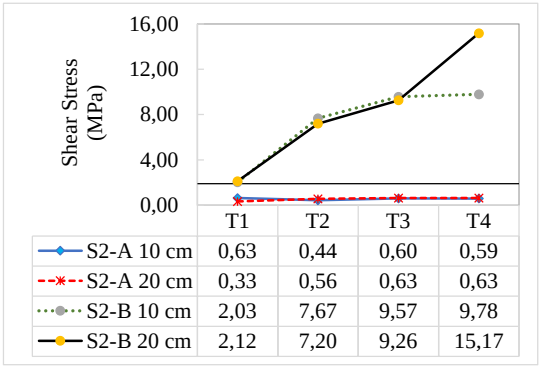


| | T1 | T2 | T3 | T4 |
|---|---|---|---|---|
| S2-A 10 cm | 0,63 | 0,44 | 0,60 | 0,59 |
| S2-A 20 cm | 0,33 | 0,56 | 0,63 | 0,63 |
| S2-B 10 cm | 2,03 | 7,67 | 9,57 | 9,78 |
| S2-B 20 cm | 2,12 | 7,20 | 9,26 | 15,17 |

(a2) S2 (L2T2G1-1)

Fig.5a Maximum shear stress of abutments (Type A and Type B)

Moreover, it is depicted that this type of input motion generally increases the shear stress on a vertical wall of the abutment. The result is higher than the maximum elastic limit of 1.9 MPa, and a crack occurs. While the input earthquake motion was applied at the bottom of all substructures, shear stress for all types of abutments is less than its limit.

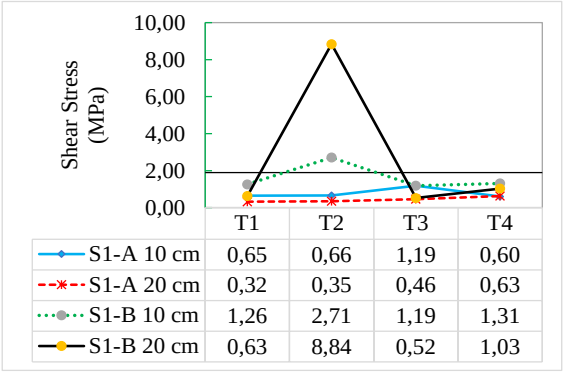


| | T1 | T2 | T3 | T4 |
|---|---|---|---|---|
| S1-A 10 cm | 0,65 | 0,66 | 1,19 | 0,60 |
| S1-A 20 cm | 0,32 | 0,35 | 0,46 | 0,63 |
| S1-B 10 cm | 1,26 | 2,71 | 1,19 | 1,31 |
| S1-B 20 cm | 0,63 | 8,84 | 0,52 | 1,03 |

(b1) S1 (L2T2G1-2)

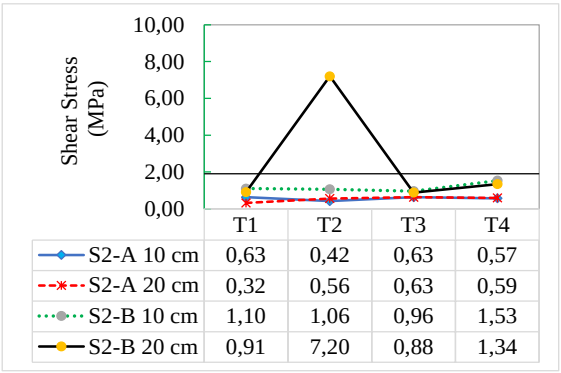


| | T1 | T2 | T3 | T4 |
|---|---|---|---|---|
| S2-A 10 cm | 0,63 | 0,42 | 0,63 | 0,57 |
| S2-A 20 cm | 0,32 | 0,56 | 0,63 | 0,59 |
| S2-B 10 cm | 1,10 | 1,06 | 0,96 | 1,53 |
| S2-B 20 cm | 0,91 | 7,20 | 0,88 | 1,34 |

(b2) S2 (L2T2G1-2)

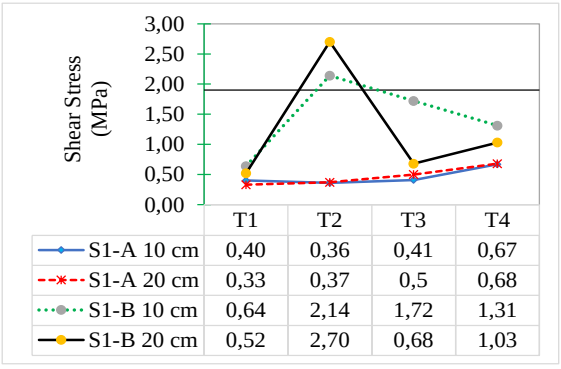


| | T1 | T2 | T3 | T4 |
|---|---|---|---|---|
| S1-A 10 cm | 0,40 | 0,36 | 0,41 | 0,67 |
| S1-A 20 cm | 0,33 | 0,37 | 0,5 | 0,68 |
| S1-B 10 cm | 0,64 | 2,14 | 1,72 | 1,31 |
| S1-B 20 cm | 0,52 | 2,70 | 0,68 | 1,03 |

(c1) S1 (L2T2G1-3)

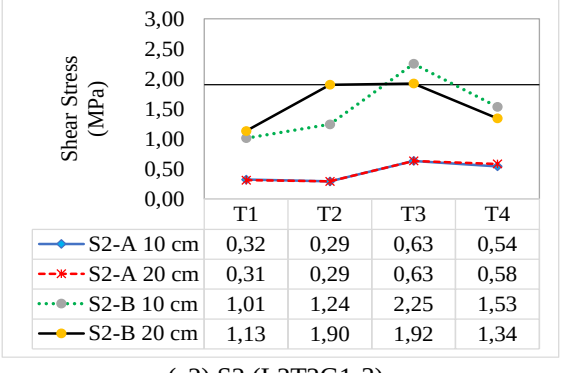


| | T1 | T2 | T3 | T4 |
|---|---|---|---|---|
| S2-A 10 cm | 0,32 | 0,29 | 0,63 | 0,54 |
| S2-A 20 cm | 0,31 | 0,29 | 0,63 | 0,58 |
| S2-B 10 cm | 1,01 | 1,24 | 2,25 | 1,53 |
| S2-B 20 cm | 1,13 | 1,90 | 1,92 | 1,34 |

(c2) S2 (L2T2G1-3)

Fig.5b,5c Maximum shear stress of abutments (Type A and Type B)

### 4.3 Response Stresses of Abutments

The response stress of each abutment was also analyzed in this research. The allowable flexural compressive stress of concrete is determined as 10 MPa, as shown in Table 2. In these numerical simulations, the response stress for each type of abutment is depicted in Fig. 6.

The diverse effect of seismic ground accelerations on each type of abutment and position can be seen in those results. The smallest response stress is figured out for bridge Type A with all types of abutments in the gap of 20 cm. Besides, the response stress of abutment Type 4 with a gap of 10 cm and 20 cm is better than other types, which is generally less than the allowable limit. It corresponds that this abutment can resist the flexural load due to strong ground motion.

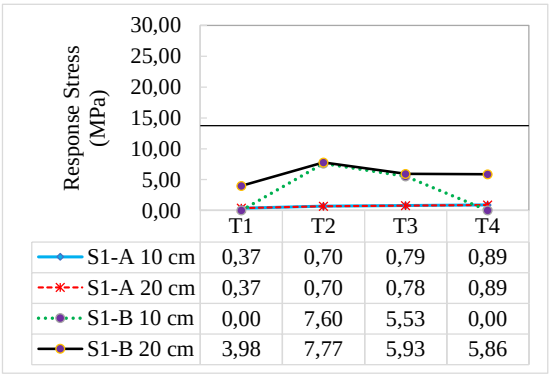


| | T1 | T2 | T3 | T4 |
|---|---|---|---|---|
| S1-A 10 cm | 0,37 | 0,70 | 0,79 | 0,89 |
| S1-A 20 cm | 0,37 | 0,70 | 0,78 | 0,89 |
| S1-B 10 cm | 0,00 | 7,60 | 5,53 | 0,00 |
| S1-B 20 cm | 3,98 | 7,77 | 5,93 | 5,86 |

(a1) S1 (L2T2G1-1)

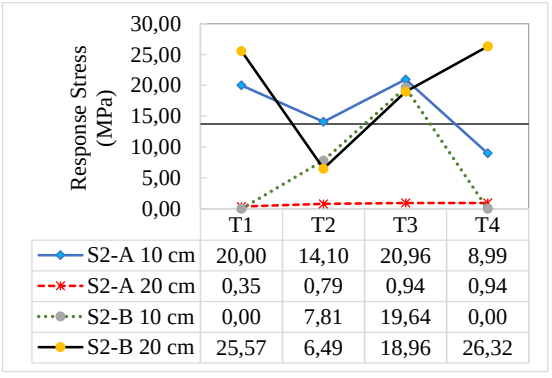


| | T1 | T2 | T3 | T4 |
|---|---|---|---|---|
| S2-A 10 cm | 20,00 | 14,10 | 20,96 | 8,99 |
| S2-A 20 cm | 0,35 | 0,79 | 0,94 | 0,94 |
| S2-B 10 cm | 0,00 | 7,81 | 19,64 | 0,00 |
| S2-B 20 cm | 25,57 | 6,49 | 18,96 | 26,32 |

(a2) S2 (L2T2G1-1)

Fig.6a Maximum response stress of abutments (TypeA and Type B)

For a bridge with a gap of 10 cm, other types of abutments including Type 1, Type 2, and Type 3 cannot resist the flexural load. However, when the gap is installed to be 20 cm, the response stress is less than the allowable stress for the left abutment.

Otherwise, when input seismic motions are applied at the bottom of the pier (Type B), the response stress is larger than Type A.

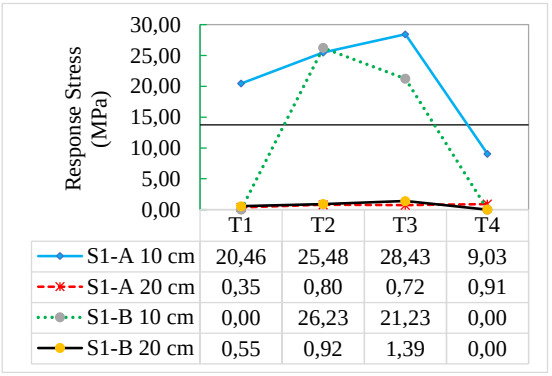


| | T1 | T2 | T3 | T4 |
|---|---|---|---|---|
| S1-A 10 cm | 20,46 | 25,48 | 28,43 | 9,03 |
| S1-A 20 cm | 0,35 | 0,80 | 0,72 | 0,91 |
| S1-B 10 cm | 0,00 | 26,23 | 21,23 | 0,00 |
| S1-B 20 cm | 0,55 | 0,92 | 1,39 | 0,00 |

(b1) S1 (L2T2G1-2)

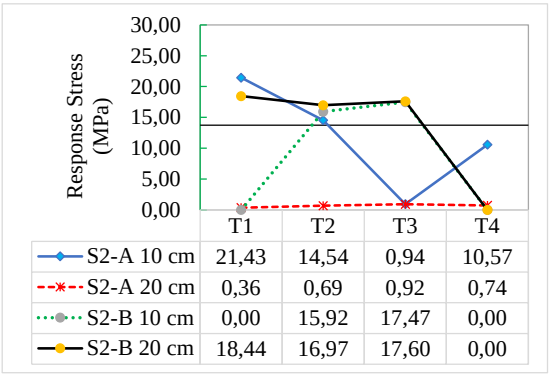


| | T1 | T2 | T3 | T4 |
|---|---|---|---|---|
| S2-A 10 cm | 21,43 | 14,54 | 0,94 | 10,57 |
| S2-A 20 cm | 0,36 | 0,69 | 0,92 | 0,74 |
| S2-B 10 cm | 0,00 | 15,92 | 17,47 | 0,00 |
| S2-B 20 cm | 18,44 | 16,97 | 17,60 | 0,00 |

(b2) S2 (L2T2G1-2)

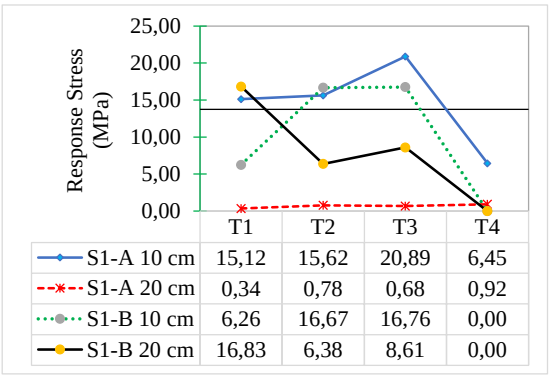


| | T1 | T2 | T3 | T4 |
|---|---|---|---|---|
| S1-A 10 cm | 15,12 | 15,62 | 20,89 | 6,45 |
| S1-A 20 cm | 0,34 | 0,78 | 0,68 | 0,92 |
| S1-B 10 cm | 6,26 | 16,67 | 16,76 | 0,00 |
| S1-B 20 cm | 16,83 | 6,38 | 8,61 | 0,00 |

(c1) S1 (L2T2G1-3)

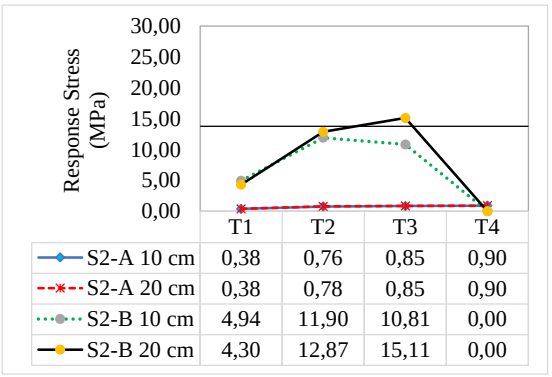


| | T1 | T2 | T3 | T4 |
|---|---|---|---|---|
| S2-A 10 cm | 0,38 | 0,76 | 0,85 | 0,90 |
| S2-A 20 cm | 0,38 | 0,78 | 0,85 | 0,90 |
| S2-B 10 cm | 4,94 | 11,90 | 10,81 | 0,00 |
| S2-B 20 cm | 4,30 | 12,87 | 15,11 | 0,00 |

(c2) S2 (L2T2G1-3)

Fig.6b, 6c Maximum response stress of abutments (Type A and Type B)

### 4.4 Horizontal Displacement of Abutments

Figs. 7(a) through Figure 7(f) show the maximum horizontal displacement at the top of the parapet wall, with the position of the abutment on the left and right side as depicted in Figure 1. The small and large displacements are determined by the ratio of 0.009 and 0.025, which are calculated by the ratio between displacements at the top of the abutment (Δ) to the height of abutment (H), Δ/H, respectively [10]. Horizontal displacement to the left and right side of abutments is figured out by positive and negative values.

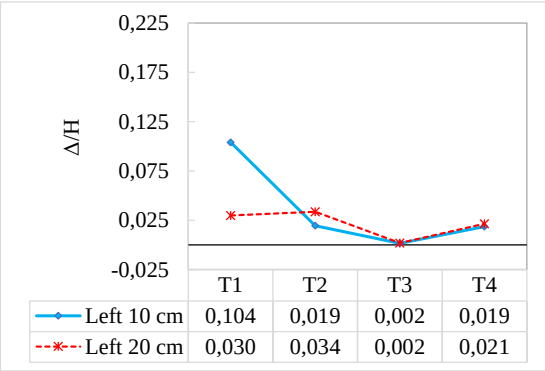


(a) S1 (L2T2G1-1)

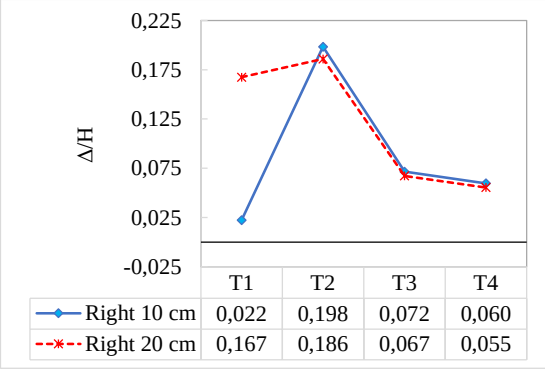


(b) S2 (L2T2G1-1)

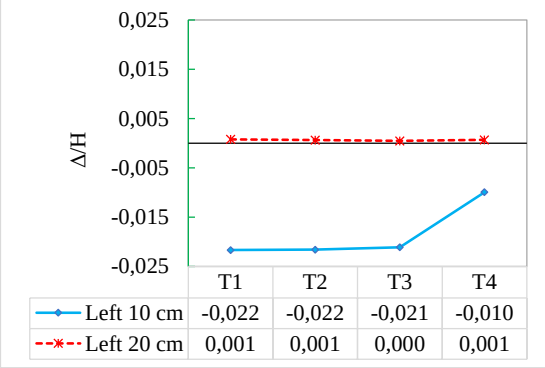


(c) S1 (L2T2G1-2)

Fig. 7a, 7b, 7c Maximum horizontal displacement at the top of abutments (Type B)

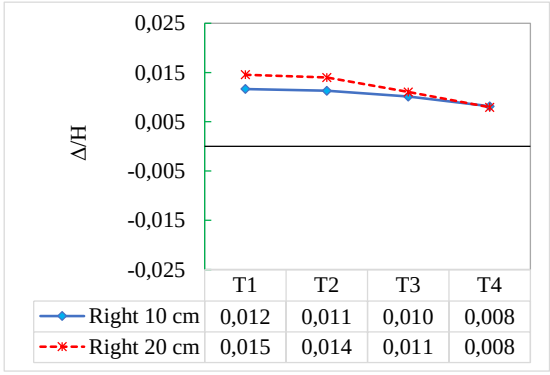


(d) S2 (L2T2G1-2)

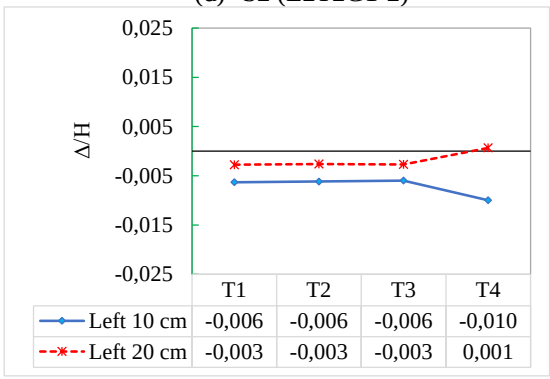


(e) S1 (L2T2G1-3)

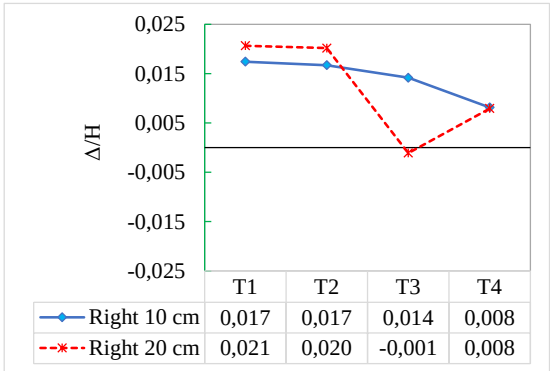


(f) S2 (L2T2G1-3)

Fig. 7d, 7e, 7f Maximum horizontal displacement at the top of abutments (Type B)

From those simulations, it can be seen that large-displacement occur at the top of abutment with seismic motion input of L2T2G1-1, as shown in Figure 7(a) and (7b). However, the reverse effect occurs on abutment with ground acceleration input of L2T2G1-2 and L2T2G1-3.

## 5. CONCLUSIONS

The dynamic responses of concrete girder bridges were investigated. Comparison study will be taken for different position of input ground acceleration, which was applied horizontally at the bottom of the pier and abutments as Type A, and at

the bottom of the pier as Type B. Level 2 Type 2 with ground Type I of seismic ground accelerations according to JSHB (Japanese Specifications for Highway Bridges) were simulated and discussed. The effect of earth pressure during the earthquake was also taken into account. The conclusions of this research are given below.

1. Installation of different abutment modeling approaches has a significant effect on its predominant mode.
2. Input seismic motion at the bottom of the pier (Type B) generally increases the shear stress on a vertical wall of abutment and resulting in cracks. While the shear stress for all types of abutments is less than its limit for Type A.
3. Abutment Type 4 with a gap of 10 cm and 20 cm has the lowest response stress comparing to other types, which is less than the allowable limit. This result corresponds that this abutment can resist the flexural load due to strong ground motion.
4. The response stress of abutment with 20 cm of a gap is less than the gap of 10 cm.
5. The effect of input seismic motions is different on its horizontal displacement of abutment for Type A.

## 6. ACKNOWLEDGMENTS

The authors greatly indebt to “Junior Research Grant (HPP) 2020” from Research and Community Service Institutions (LPPM) Universitas Brawijaya for providing financial support through this research. Special thanks to the Civil Engineering Department, Universitas Brawijaya for supporting this opportunity.

## 7. REFERENCES

[1]. Aviram, A.; Mackie, K.R.; and Stojadinovic, B., Effect of Abutment Modeling on the Seismic Response of Bridge Structures, Earth Eng & Eng Vib., Vol. 7, Issue 4, 2008, pp. 395-402.

[2]. Setyowulan, D.; Hamamoto, T.; and Yamao, T., Elasto-Plastic Behavior of 3-Dimensional Reinforced Concrete Abutments Considering the Effect of the Wing Wall, International Journal of Civil Engineering and Technology (IJCIET), Vol. 5, Issue 11, 2014, pp. 97-113.

[3]. Susanti, L., Setyowulan, D., Wijaya, M.N., Experimental Investigation on Behavior of RC Parapet Wall of Abutment Under Collision, International Journal of Civil Engineering and Technology (IJCIET), Vol. 9, Issue 9, 2019, pp. 1831-1838.

[4]. Yamao, T.; Kawachi, A.; and Tsutsui, M., Static and Dynamic Behaviour of A Parapet Wall of the Abutment, Proceeding of the 11th International Conference on Steel, Space and Composite Structures, Qingdao (China), 2012.

[5]. Hamamoto, T., Yamao, T., Setyowulan, D., Analytical Study on Seismic Response Reduction for PC Bridge: Effects of Cost on a Proposed Seismic Reinforcement Method Due to Collision, Journal of Civil, Construction and Environmental Engineering (JCEE), Vol. 5, Issue 3, 2020, pp. 57-66.

[6]. Setyowulan, D., Yamao, T., Yamamoto, K., and Hamamoto, T., Investigation of Seismic Response on Girder Bridges: The Effect of Displacement Restriction and Wing Wall Types, Procedia - Social and Behavioral Sciences, Vol. 218, 2016, pp. 104 – 117.

[7]. Dassault Systems Simulia Corp., ABAQUS/CAE User’s Manual 6.11, 2011.

[8]. Mokhatar, S.N.; and Abdullah, R., Computational Analysis of Reinforced Concrete Slabs Subjected to Impact Loads, International Journal of Integrated Engineering, Vol. 4, Issue 2, 2012, pp. 70-76.

[9]. Japan Road Association, Specifications for Highway Bridges Part V: Seismic design, 2002.

[10]. Ahmed, A., Modeling of A Reinforced Concrete Beam Subjected to Impact Vibration Using ABAQUS, International Journal of Civil and Structural Engineering, Vol. 4, Issue 3, 2014, pp. 227-236.